Exploiting P-chemistry to modulate the thermally activated delayed fluorescence of organic fluorophores

Nicolas Ledos, Denis Jacquemin, Pierre-Antoine Bouit, Muriel Hissler

Dyes and Pigments 224 (2024) 111978

Contents lists available at ScienceDirect

Dyes and Pigments

journal homepage: www.elsevier.com/locate/dyepig

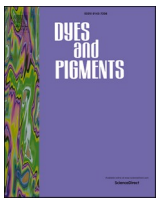

Exploiting P-chemistry to modulate the thermally activated delayed fluorescence of organic fluorophores

Nicolas Ledos [a], Denis Jacquemin [b,c,**], Pierre-Antoine Bouit [a,*], Muriel Hissler [a,***]

[a] Univ Rennes, CNRS, ISCR - UMR 6226, F-35000, Rennes, France
[b] Nantes Université, CNRS, CEISAM UMR 6230, F-44000, Nantes, France
[c] Institut Universitaire de France (IUF), F-75005, Paris, France

ARTICLE INFO

Keywords:
Fluorophore
Delayed fluorescence
Organophosphorus

ABSTRACT

A series of six organophosphorus emitters featuring phosphinate and phosphinic acid groups as electron-accepting moieties coupled to various arylamine-based donor groups has been synthesized and fully characterized. Their photophysical properties were extensively investigated and the structure property relationships were rationalized using TD-DFT calculations. This work demonstrates that a judicious choice of the P-substituent allows promoting or suppressing the thermally activated delayed fluorescence (TADF). This investigation also offers interesting perspectives toward the preparation of stimuli-responsive TADF derivatives.

1. Introduction

Thermally activated delayed fluorescence (TADF) is a photophysical phenomenon observed in compounds displaying a small singlet–triplet energy gap (ΔE_{ST}). This characteristic allows triplet excitons to convert back to singlet ones through reverse intersystem crossing (RISC) [1]. Adachi et al. successfully used TADF emitters to surpass the 5 % theoretical limit of fluorescent Organic Light-Emitting Diodes (OLEDs) [2]. Nowadays, TADF materials have gained considerable attention, and numerous examples of TADF-based OLEDs display External Quantum Efficiency (EQE) above 30 % [3–8]. Additionally, the relatively long luminescence lifetime of these emitters, due to the involvement of triplet states, provide advantages for other applications, such as organo-photo-catalysis and photodynamic therapy [9,10]. One approach to achieve TADF is to design Donor-Acceptor (D-A) systems where the Highest Occupied Molecular Orbital (HOMO) and Lowest Unoccupied Molecular Orbital (LUMO) are spatially separated, the small overlap leading to trifling ΔE_{ST} [11]. Currently, there is a wide variety of donor groups available for building TADF emitters, while the number of acceptor groups is comparatively limited [12]. Among the acceptors, the phosphine oxide moiety is one of them [13], as its intrinsic tetrahedral geometry associated with the presence of electronegative O-atom makes it particularly suitable for designing TADF emitters. This specific geometry favors high triplet energy by inhibiting the conjugation between different substituents of the P-atom. Furthermore, such geometry efficiently prevents π-π stacking and can be used to introduce significant steric constraints. These characteristics limit non-radiative pathways in the solid-state, resulting in an overall improved Photoluminescence Quantum Yield (PLQY). However, the field of organophosphorus chemistry offers an almost unlimited array of variations of the phosphine oxide moiety. Until now, only the P(=O)-Ph group has been employed in the TADF line of research. Increasing the variety of accepting units to build TADF compounds is essential to develop new TADF emitters and expand the scope of applications for example in biophotonic (if used in photodynamic therapy for example) or to develop novel hybrid material for example for application in photocatalysis.

To address this issue, we started from a phosphine oxide scaffold known in the literature for its TADF properties (**A** and **B**), and we designed a full family of emitters by varying the phosphorous environment (Fig. 1) [14–20]. Instead of the P(=O)Ph group, we substituted it with methylphosphinate (POOMe) or phosphinic acid(POOH) and explored the photophysics of the resulting compounds. In this article, we present the synthesis of six novel emitters and conduct a comprehensive physico-chemical characterization using a combined experimental-theoretical approach, with a particular emphasis on the

* Corresponding author.
** Corresponding author. Nantes Université, CNRS, CEISAM UMR 6230, F-44000, Nantes, France.
*** Corresponding author.
E-mail addresses: Denis.Jacquemin@univ-nantes.fr (D. Jacquemin), pierre-antoine.bouit@univ-rennes.fr (P.-A. Bouit), muriel.hissler@univ-rennes.fr (M. Hissler).

https://doi.org/10.1016/j.dyepig.2024.111978
Received 4 December 2023; Received in revised form 15 January 2024; Accepted 22 January 2024
Available online 1 February 2024

optical properties. In particular, we show that the TADF behavior of the compound can be modulated and even turned off depending on the P-environment.

2. Synthesis

All the phosphinic acid-based fluorophores **4–6** were successfully synthesized in high yields using a Pd-catalyzed approach developed by Botez et al. (Fig. 2)[21]. This synthetic pathway eliminates the need for halogeno-phosphines, making the synthesis safer and more environmentally friendly. All these compounds display limited solubility in most organic solvents. However, upon basic treatment with triethylamine, their triethylammonium salt display good solubility allowing their easy purification by silica gel chromatography. The phosphinic acid can be regenerated using hydrochloric acid. The corresponding phosphinates **7–9** were also synthesized in good yield through N, N′-Dicyclohexylcarbodiimide (DCC) coupling with methanol(Fig. 2). All compounds were fully characterized by multinuclear NMR and mass spectrometry. Having in hands these compounds afford the possibility for a rational study of the impact of the P-environment on the photophysical properties, including the TADF efficiencies.

3. Optical properties

The optical properties of compounds **4–9** were measured in diluted toluene solutions (C ≈ 10^{-5} mol L^{-1}). First, the UV–visible absorption spectra of the entire family were investigated (Fig. 3). All compounds exhibit multiple absorption bands, mainly in the UV range. Compounds with the same electron-donating groups display very similar properties **4**, **6**, **7** and **9** composed of DMAc or PXZ groups, display absorption spectra with two broad bands. The first band is intense (ε > 10 000 L mol^{-1} cm^{-1}) with a maximum at ca. 290 nm and 324 nm for DMAc and PXZ respectively, associated with a π-π* transition located on the electron-donating groups. This band is followed by a weak shoulder (ε < 3000 L mol^{-1} cm^{-1}) ranging from 340 to 390 nm for DMAc and 360–420 nm for PXZ, associated with a charge transfer (CT) from DMAc/PXZ to the PO function. The same behavior is reported by Duan et al. for **A-B** emitters [14,15]. Emitters **5** and **8**, containing tBu_2Cbz groups, display absorption spectra with three bands characteristic of π-π* transitions located on the tBu_2Cbz groups. No band with a pure CT state seems present in these two molecules (see also theoretical calculations below).

All derivatives are luminescent, and their emission spectra span from violet to blue-green. Emitters with tBu_2Cbz groups emit at the most blueshifted wavelengths (λ_{max}(**5**) = 390 nm and λ_{max}(**8**) = 380 nm) due to the lack of marked CT character. Emitters containing DMAc groups display luminescence in the blue region: λ_{max}(**4**) = 446 nm and λ_{max}(**7**) = 428 nm, similar to their analog bearing a POPh group (compound **A**) [15]. Compound with PXZ groups exhibit blue-green emission: λ_{max}(**6**) = 491 nm and λ_{max}(**9**) = 475 nm, again rather similar to their POPh counterpart **B** [14]. Additionally, compound **9**, featuring a POOH function, shows the most redshifted emission. Hence, the order of electro attracting power for the different PO functions seems to be: POPh ≈ POOMe < POOH. The photoluminescence quantum yields of all compounds were determined under both aerated and inert conditions to investigate any potential contribution of the triplet state in the radiative pathway.

To gain deeper insights into the spectroscopic properties, DFT and TD-DFT calculations were carried out to understand the differences between **5** and **6** (see the ESI for details). In **5**, the dihedral angles between the phenyl ring attached to the P atom and the donor groups are ca. 50°, allowing for a significant communication between the two moieties. Consequently, the resulting state shows a bright nature with a moderate yet significant CT character with the phosphorous acting as the acceptor (mostly in red in Fig. 4), the oscillator strength being large (f = 0.772 at TD-DFT level). Le Bahers' CT model [22] predicts the transfer of 0.85 e over 1.61 Å, but the CT distance is likely slightly underestimated given the "V-shape" of the system. The second transition of **5** presents a rather similar nature, yet with a smaller oscillator strength. In **6** (Fig. 4), the uncoupling between the two donor units and the central accepting core creates two (nearly) degenerate and dark transitions, both of clear CT character, with a CT distance of ca. 2.94 Å.

To have a general overview of the absorption spectra, we have simply convoluted the TD-DFT stick data obtained with a standard solvation model with a Gaussian broadening function of HWHM of 0.10 eV. As can be seen in Fig. S3., and unsurprisingly, the agreement with experiment is qualitative only. While the intense band of **5** above 300 nm is reproduced, it is too blueshifted. Likewise, the less intense and higher-energy band of **6** is found, but the intensity of the redshifted peak corresponding to the CT (at ca. 335 nm in the calculations) is clearly strongly undershot. There are several reasons to this: *i*) the solvent model is not ideal for CT; *ii*) vibrational effects are neglected, which should greatly affect the lowest transitions of **6** due to Herzberg-Teller effects; and *iii*) TD-DFT is limited by the quality of the selected functional. In an effort to improve the simulations, we have determined vertical absorption and emission for the lowest transition accounting for state-specific solvent effects [23], and including coupled-cluster (CC2) corrections. Table S1 in the ESI provides the theoretically computed vertical transition wavelengths, as well as, the 0-0 energies. These energies can be directly compared to experiment and theory return 3.29 eV for **5**, corresponding to an absorption-emission crossing point at 376 nm, only slightly redshifted compared to experiment. Both the absorption and emission of **5** are associated to large oscillator strengths, consistent with the measurements. In contrast in **6**, there is significant redshift of all computed values as compared to **5**, in line with experiment. One also notices that the oscillator strengths associated to both absorption and emission are very small for **6**, which indicates poorer absorptivity and radiative rate, respectively, again consistent with the experimental trends detailed in Table 1.

Compounds **4**, **6**, **7**, and **9** exhibit similar experimental quantum yields, ranging from 7 % to 13 %, under aerated conditions, whereas compounds **5** and **8** display higher quantum yields of 46 % and 47 %,

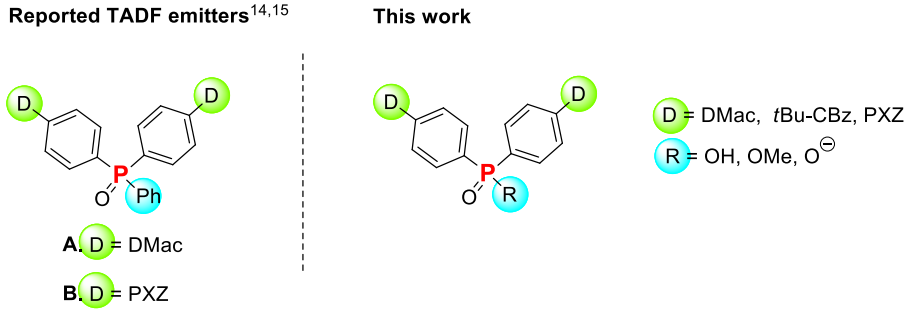

Fig. 1. Structure of reported phosphine oxide based TADF emitters and compound studied in this article.

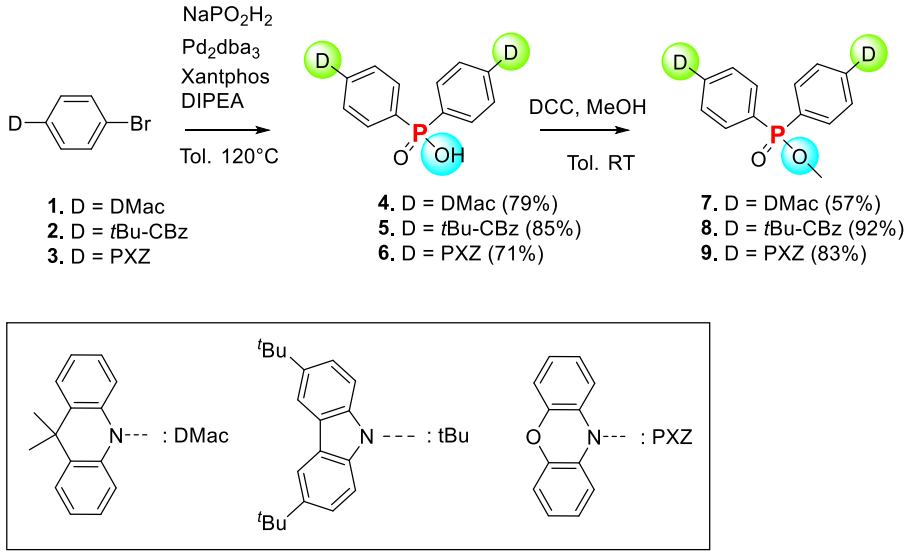

Fig. 2. Synthetic access to **4–9** and their respective reaction yield.

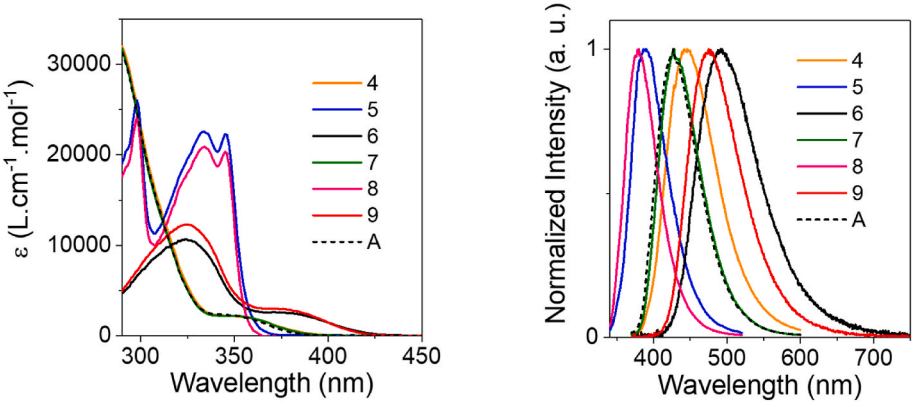

Fig. 3. Absorption and fluorescence spectra of emitters **4–9**.

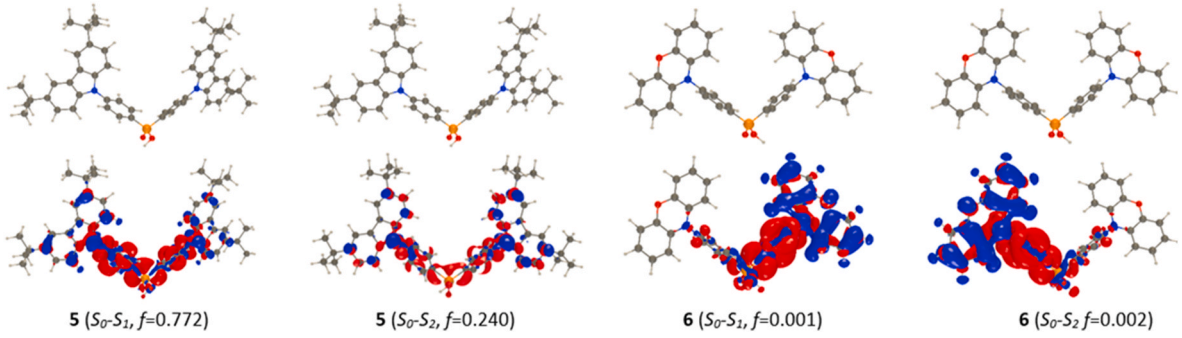

Fig. 4. Structure (top) and electron density difference (EDD) plot (bottom) corresponding to the absorption of **5** and **6**. The blue and red lobes correspond to decrease and increase of electron density, respectively. Oscillator strengths are indicated. Contour threshold 0.001 au.

respectively. This disparity is attributed to the different nature of transitions involved in fluorescence: for compounds **5** and **8**, luminescence arises from a dipole-allowed π-π* transition with a limited CT character, whereas for compounds **4**, **6**, **7**, and **9**, the luminescence originates from an almost dark transition with a pure CT nature, associated with a very small oscillator strength (see Fig. 4). Moving from aerated to inert conditions leads to a remarkable increase in all quantum yields. While a slight rise is observed for compounds **5**, **7**, and **8**, a much more significant increase is evident for compounds **4**, **6**, and **9**. Remarkably, for compound **6**, the quantum yield rises from 11 % to 67 %. This strong dependence on the presence of oxygen for emitters **4**, **6**, and **9** suggests the involvement of a triplet state in their luminescence. To gain deeper insights into these different responses, time-resolved spectroscopic studies have been conducted.

Time-resolved spectroscopic studies have unveiled that emitters **4**, **6**, and **9** exhibit a long-lived emissive component ranging from

Table 1
Optical properties of emitters **4–9** in toluene.

Cpd	λ_{max}abs (nm)	ε (L.mol^{-1}.cm^{-1})	λ_{max}em (nm)	Φ_{PL}(A) aerated (±10 %)	Φ_{PL}(A) inert (±10 %)
4	290, 350	32 000, 2000	446	0.13[a]	0.30[a]
5	298	26 000	390	0.46[b]	0.53[b]
6	324, 380	11 000, 3000	491	0.11[a]	0.67[a]
7	290, 350	32 000, 2000	428	0.12[a]	0.20[a]
8	298	24 000	380	0.47[b]	0.53[b]
9	324, 380	12 000, 3000	475	0.07[a]	0.33[a]

[a] Absolute quantum yield.
[b] PLQY determined relative to quinine sulfate.

microseconds to tens of microseconds (see Table 2 and Fig. S2). These long-lived components are coexisting with the prompt fluorescence of those emitters. For this reason, and by analogy with reported compounds **A** – **B** discussed above [14,15], this behavior has been ascribed to TADF.

To understand the absence of TADF signatures in compounds **5**, **7**, and **8**, we conducted an experimental determination of the ΔE_{ST}, Fig. S1. Emitters **5** and **8** possess a very large ΔE_{ST} (0.55 and 0.61 eV respectively). This is linked with the absence CT in absorption and explain why they do not display any TADF behaviour — the EDD of the lowest triplet of **5** is indeed localized (Fig. S6). Indeed, the Donor-Acceptor pairs tBu_2Cbz/POOH and tBu_2Cbz/POOMe are not electronically strong enough to induce TADF properties, at least on the geometries of the systems under investigation. In contrast, emitters **6** and **9** display a low ΔE_{ST} (0.15 and 0.20 eV respectively) consistent with a clear CT character. The PXZ group is the strongest donor in the series, leading both emitters to display TADF behaviour. It is also noteworthy that the electron-attracting effect of the POOH group, stronger than that of the POOMe group, results in a lower ΔE_{ST}. Emitters **4** and **7**, which incorporate DMAc groups, exhibit CT bands in absorption and possess the lowest ΔE_{ST} values in series (0.03 and 0.09 eV respectively). However, despite these low ΔE_{ST} values, only emitter **4** displays TADF properties.

Such observations were corroborated by theoretical calculations. Indeed, on the S1 optimal geometry of **5**, SCS-CC2/*aug*-cc-pVDZ returns two triplet states below the lowest singlet with respective ΔE_{ST} (of 0.41 eV and 0.05 eV, the second one therefore showing a very small separation favorable for ISC, but not RISC and therefore not TADF. The value of 0.41 eV is reasonably fitting the experimental measurement of 0.55 eV. In **6**, theory foresees an almost perfect alignment between the lowest singlet and triplet states at 2.71 eV each, i.e., a negligible ΔE_{ST}, consistent with the small value measured experimentally (in a different environment, which can affect the conformation of the system).

To elucidate these disparities, the photophysical rate constants involved in the TADF process have been calculated (Table 3, see details in the ESI). Emitter **6** exhibits more efficient ISC, DF, and RISC than **9**. The constants k_{DF} and k_{ISC} are up to 30 times higher, and k_{RISC} is five times higher as well for emitter **6**. Additionally, the D-A pair POPh-PXZ (emitter **B**) showcases emission wavelengths similar to the POOMe-PXZ pair (emitter **9**). Therefore, these two donor-acceptor pairs could be considered electronically equivalent. However, their TADF rate constants differ significantly, with emitter **B** displaying notably higher values (particularly k_{ISC}) compared to emitter **9**. The presence of the POPh group seems more suitable to provide TADF properties than the POOMe group, an analysis supported by the characteristics of emitters **4**, **7**, and **A**. Both compounds **4** and **B** exhibit TADF properties, whereas compound **7**, which contains a POOMe group, does not. This discrepancy suggests that the k_{ISC} constant of compound **7** is likely insufficient to induce delayed fluorescence.

This study shows that modifying the P environment through formation of an alkyl phosphinate leaves intact the TADF character previously observed on POPh analogs. This observation is of high interest as P-functionalization is frequently used for material structuration [24], or bioconjugation [25].

Among the P-modifications that can be easily perform on pi-conjugated phosphinic acids, deprotonation appear to strongly affect its optical properties [26]. Investigation of the spectroscopic properties of the anionic phosphinate derivatives of compounds **4**, and **6** was thus conducted to check its impact on the TADF behavior of these systems (Fig. 5 and Fig. S3). Measurements were carried out in solution by dissolving compounds **4** and **6** in a toluene solution containing triethylamine (1 % by volume). Under basic conditions, the absorption spectra of both **4** and **6** undergo significant changes (Fig. 5). For emitter **4** and **6**, the broad band attributed to transitions centered on the arylamine remains unaltered, but the CT-related band disappears. The emissions of **4** and **6** also shift towards the blue under basic conditions (Fig. 5). We underline that theory does not reproduce the fluorescence blueshift from neutral to deprotonated **6**, see the SI, which we attribute to the difficulty of obtaining very accurate energies for anionic species with the selected protocol. In the case of compound **4**, the emission maximum shifts from 446 nm to 402 nm. As for compound **6**, the emission maximum shifts from 491 nm to 433 nm. In other words, the deprotonation of the POOH group doesn't influence the electron properties of the arylamine groups, but totally quench the bands with CT characteristics. This is attributed to the transformation from an electron acceptor to an electron donor group while switching from POOH to a POO^- function. Indeed, TD-DFT confirm that the deprotonated form of **6** displays large twist angles and nearly-degenerated transitions as the parent compounds, but these transitions have now a purely local character, as the PO_2^- group cannot act as an acceptor moiety (Fig. S4). For emitters **4** and **6**, the CT transition is responsible for their fluorescent and delayed fluorescent properties, which are also modified under basic conditions. Consequently, emitters **4** and **6** lose their TADF properties under basic conditions. Indeed, the luminescence decay only shows prompt fluorescence with similar lifetime ($\tau \sim 2.5$ ns) and PLQY (0.07 vs 0.08) in presence and in absence of oxygen (Fig. S4). SCS-CC2 calculations confirm that in the deprotonated form of **6**, there is only one triplet below the singlet state, but with a large gap of −0.57 eV.

Thus, emitters **4** and **6** display a very peculiar behaviour of switchable fluorescence/delayed fluorescence properties trigger by pH. Such property can be of high interest to design stimuli responsive systems.

Table 2
Fluorescence and delayed fluorescence lifetimes of emitters **4–9** in toluene. Estimation of their $E(S_1)$, $E(T_1)$ et ΔE_{ST}.

	τ_{PF} (ns)	τ_{DF} (µs)	$E(S_1)$ (eV)	$E(T_1)$ (eV)	ΔE_{ST} (eV)
4	16.2	2.5	3.15	3.12	0.03
5	4.7	–	3.52	2.97	0.55
6	24.8	12.4	2.88	2.73	0.15
7	8.7	–	3.21	3.12	0.09
8	4.0	–	3.59	2.99	0.61
9	20.9	52.8	2.94	2.74	0.20

4. Conclusion

A new series of organophosphorus emitters **4–9** featuring phosphinate and phosphinic acid groups as electron-accepting moieties coupled to various arylamine-based donor groups has been synthesized. Notably, these derivatives were prepared without the use of toxic halogenophosphines. In total, six novel compounds were obtained a fully characterized, and their photophysical properties were extensively investigated and the structure property relationships were rationalized. This work demonstrates that a judicious choice of the P-substituent (POOH, POPh, POOMe, and POO^- functionalities) allows to preserve or totally suppress the TADF. This study paves the way toward the preparation of novel stimuli-responsive TADF derivatives [27–29] and their

Table 3
Photophysical properties of TADF emitters **4**, **6**, **9**.

	λ_{max}em (nm)	Φ_{PL} (±10 %)	Φ_{PF}/Φ_{DF} (%/%)	τ_{PF} (ns)	τ_{DF} (μs)	k_{PF} (x10^6 s^{-1})	k_{DF} (x10^3 s^{-1})	k_{ISC} (x10^6 s^{-1})	k_{RISC} (x10^4 s^{-1})
4	446	0.30	19/11	16.2	2.5	11.7	44.0	4.3	6.9
6	491	0.67	10/57	24.8	12.4	40.3	46.0	34.3	30.8
9	475	0.33	3/30	20.9	52.8	1.4	5.7	1.3	6.1

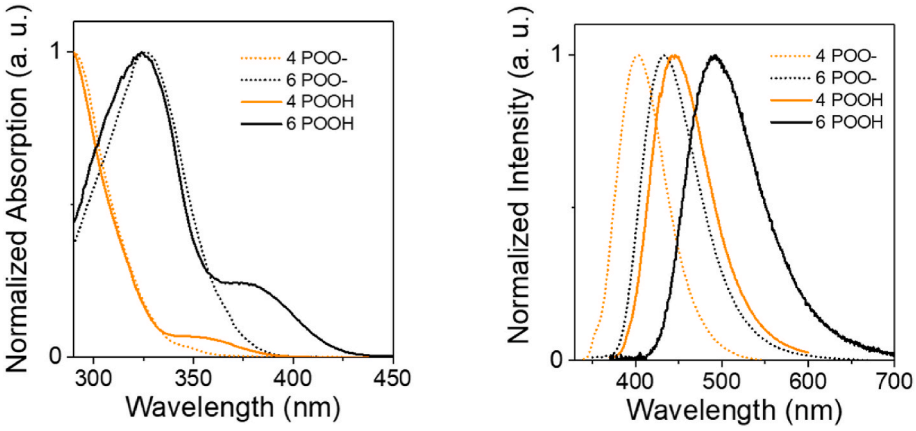

Fig. 5. Absorption and fluorescence spectra of emitters **4** and **6** in neutral (labeled POOH) and basic media (labeled POO-) (top).

use for new developments in optoelectronics, in biophotonics or catalysis.

CRediT authorship contribution statement

Nicolas Ledos: Writing – original draft, Investigation. **Denis Jacquemin:** Writing – review & editing, Investigation. **Pierre-Antoine Bouit:** Writing – review & editing, Conceptualization. **Muriel Hissler:** Funding acquisition, Conceptualization.

Declaration of competing interest

The authors declare that they have no known competing financial interests or personal relationships that could have appeared to influence the work reported in this paper.

Data availability

Data will be made available on request.

Acknowledgments

This work is supported by the Ministère de la Recherche et de l'Enseignement Supérieur, the CNRS, the Région Bretagne, the French National Research Agency (ANR Fluohyb ANR-17-CE09-0020), the China-French associated international laboratory in "Functional Organophosphorus Materials", the GDR Phosphore. NL thanks the Région Bretagne for PhD grant. DJ is indebted to the CCIPL computational center installed in Nantes for generous allocations of computational time.

Appendix A. Supplementary data

Supplementary data to this article can be found online at https://doi.org/10.1016/j.dyepig.2024.111978.

References

[1] Endo A, Sato K, Yoshimura K, Kai T, Kawada A, Miyazaki H, et al. Efficient up-conversion of triplet excitons into a singlet state and its application for organic light emitting diodes. Appl Phys Lett 2011;98:083302. https://doi.org/10.1063/1.3558906.
[2] Uoyama H, Goushi K, Shizu K, Nomura H, Adachi C. Highly efficient organic light-emitting diodes from delayed fluorescence. Nature 2012;492:234–8. https://doi.org/10.1038/nature11687.
[3] Cheng Y, Fan X, Huang F, Xiong X, Yu J, Wang K, et al. A highly twisted carbazole-fused DABNA derivative as an orange-red TADF emitter for OLEDs with nearly 40 % EQE. Angew Chem Int Ed 2022;134. https://doi.org/10.1002/ange.202212575.
[4] Hong G, Gan X, Leonhardt C, Zhang Z, Seibert J, Busch JM, et al. A brief history of OLEDs—emitter development and industry milestones. Adv Mater (Weinheim, Ger) 2021;33:2005630. https://doi.org/10.1002/adma.202005630.
[5] Kotadiya NB, Blom PWM, Wetzelaer G-JAH. Efficient and stable single-layer organic light-emitting diodes based on thermally activated delayed fluorescence. Nat Photonics 2019;13:765–9. https://doi.org/10.1038/s41566-019-0488-1.
[6] Wu S, Zhang L, Wang J, Kumar Gupta A, Samuel IDW, Zysman-Colman E. Merging boron and carbonyl based MR-TADF emitter designs to achieve high performance pure blue OLEDs**. Angew Chem Int Ed 2023;62:e202305182. https://doi.org/10.1002/anie.202305182.
[7] Xiao Y, Wang H, Xie Z, Shen M, Huang R, Miao Y, et al. NIR TADF emitters and OLEDs: challenges, progress, and perspectives. Chem Sci 2022;13:8906–23. https://doi.org/10.1039/D2SC02201J.
[8] Kim D-H, D'Aléo A, Chen X-K, Sandanayaka ADS, Yao D, Zhao L, et al. High-efficiency electroluminescence and amplified spontaneous emission from a thermally activated delayed fluorescent near-infrared emitter. Nat Photonics 2018;12:98–104. https://doi.org/10.1038/s41566-017-0087-y.
[9] Bryden MA, Zysman-Colman E. Organic thermally activated delayed fluorescence (TADF) compounds used in photocatalysis. Chem Soc Rev 2021;50:7587–680. https://doi.org/10.1039/D1CS00198A.
[10] Nguyen V-N, Kumar A, Lee MH, Yoon J. Recent advances in biomedical applications of organic fluorescence materials with reduced singlet–triplet energy gaps. Coord Chem Rev 2020;425:213545. https://doi.org/10.1016/j.ccr.2020.213545.
[11] Liang X, Tu Z, Zheng Y. Thermally activated delayed fluorescence materials: towards realization of high efficiency through strategic small molecular design. Chem Eur J 2019;25:5623–42. https://doi.org/10.1002/chem.201805952.
[12] Im Y, Kim M, Cho YJ, Seo J-A, Yook KS, Lee JY. Molecular design strategy of organic thermally activated delayed fluorescence emitters. Chem Mater 2017;29:1946–63. https://doi.org/10.1021/acs.chemmater.6b05324.
[13] Song X, Xu H. Pure-organic phosphine oxide luminescent materials. J Inform Disp 2020;21:149–72. https://doi.org/10.1080/15980316.2020.1788657.
[14] Duan C, Li J, Han C, Ding D, Yang H, Wei Y, et al. Multi-dipolar chromophores featuring phosphine oxide as joint acceptor: a new strategy toward high-efficiency blue thermally activated delayed fluorescence dyes. Chem Mater 2016;28:5667–79. https://doi.org/10.1021/acs.chemmater.6b01691.
[15] Duan C, Li Z, Zhang J, Han C, Xu H. Direct evidence of dopant-dopant synergism in efficient single-emissive-layer white thermally activated delayed fluorescence. Nano Energy 2021;89:106358. https://doi.org/10.1016/j.nanoen.2021.106358.
[16] Li Z, Duan C, Li Y, Zhang J, Han C, Xu H. Exciton engineering based on star-shaped blue thermally activated delayed fluorescence emitters for efficient white organic light-emitting diodes. J Mater Chem C 2021;9:15221–9. https://doi.org/10.1039/D1TC03779J.

[17] Liao X, Shen B, Li Y, Cheng J, Li L. Highly efficient and low efficiency roll-off single-emissive-layer white organic light emitting devices by quaternary exciplex. Dyes Pigments 2023;208:110803. https://doi.org/10.1016/j.dyepig.2022.110803.
[18] Ulukan P, Bas EE, Ozek RB, Dal Kaynak C, Monari A, Aviyente V, et al. Computational descriptor analysis on excited state behaviours of a series of TADF and non-TADF compounds. Phys Chem Chem Phys 2022;24:16167–82. https://doi.org/10.1039/D2CP01323A.
[19] Ledos N, Tondelier D, Geffroy B, Jacquemin D, Bouit P-A, Hissler M. Reaching the 5 % theoretical limit of fluorescent OLEDs with push–pull benzophospholes. J Mater Chem C 2023;11:3826–31. https://doi.org/10.1039/D3TC00245D.
[20] Phelipot J, Ledos N, Dombray T, Duffy MP, Denis M, Wang T, et al. Highly emissive layers based on organic/inorganic nanohybrids using aggregation induced emission effect. Adv Mater Technol 2022;7:2100876. https://doi.org/10.1002/admt.202100876.
[21] Botez L, de Jong GB, Slootweg JC, Deelman B-J. A direct catalytic synthesis of sodium diarylphosphinates and their corresponding acids from sodium phosphinate: a direct catalytic synthesis of sodium diarylphosphinates and their corresponding acids from sodium phosphinate. Eur J Org Chem 2017;2017:434–7. https://doi.org/10.1002/ejoc.201601222.
[22] Le Bahers T, Adamo C, Ciofini I. A qualitative index of spatial extent in charge-transfer excitations. J Chem Theor Comput 2011;7:2498–506. https://doi.org/10.1021/ct200308m.
[23] Guido CA, Chrayteh A, Scalmani G, Mennucci B, Jacquemin D. Simple protocol for capturing both linear-response and state-specific effects in excited-state calculations with continuum solvation models. J Chem Theor Comput 2021;17:5155–64. https://doi.org/10.1021/acs.jctc.1c00490.
[24] Wang Z, Gelfand BS, Baumgartner T. Dithienophosphole-based phosphinamides with intriguing self-assembly behavior. Angew Chem Int Ed 2016;55:3481–5. https://doi.org/10.1002/anie.201511171.
[25] Arribat M, Rémond E, Clément S, Lee AVD, Cavelier F. Phospholyl(borane) amino acids and peptides: stereoselective synthesis and fluorescent properties with large Stokes shift. J Am Chem Soc 2018;140:1028–34. https://doi.org/10.1021/jacs.7b10954.
[26] Turnbull JL, Benlian BR, Golden RP, Miller EW. Phosphonofluoresceins: synthesis, spectroscopy, and applications. J Am Chem Soc 2021;143:6194–201. https://doi.org/10.1021/jacs.1c01139.
[27] Song T, Liu H, Ren J, Wang Z. Achieving TADF and RTP with stimulus-responsiveness and tunability from phenothiazine-based Donor−Acceptor molecules. Adv Opt Mater 2023:2301215. https://doi.org/10.1002/adom.202301215. n/a.
[28] Li D, Yang Y, Yang J, Fang M, Tang BZ, Li Z. Completely aqueous processable stimulus responsive organic room temperature phosphorescence materials with tunable afterglow color. Nat Commun 2022;13:347. https://doi.org/10.1038/s41467-022-28011-6.
[29] Steinegger A, Klimant I, Borisov SM. Purely organic dyes with thermally activated delayed fluorescence—a versatile class of indicators for optical temperature sensing. Adv Opt Mater 2017;5:1700372. https://doi.org/10.1002/adom.201700372.